Progress In Electromagnetics Research, Vol. 111, 1–24, 2011

MODAL ANALYSIS OF BI-ISOTROPIC H-GUIDES

J. R. Canto, C. R. Paiva, and A. M. Barbosa

Instituto de Telecomunicações
Department of Electrical and Computer Engineering
Instituto Superior Técnico
Av. Rovisco Pais 1, Lisboa 1049-001, Portugal

Abstract—Using a building block approach which combines a transverse resonance method with a mode-matching technique, a rigorous analysis of a lossless bi-isotropic H-guide is presented. First, the modal equation of a parallel-plate waveguide containing the inner medium of the H-guide is obtained. Then, a mode matching technique is used to develop a full-wave analysis of the H-guide. The influence of nonreciprocity on the guidance properties of the structure is discussed.

1. INTRODUCTION

The concept of a nonreciprocal isotropic medium has been introduced by Tellegen as early as 1948. It has resurged in the mid 90's, giving rise to a major debate on whether linear bi-isotropic media can actually be nonreciprocal. In a linear bi-isotropic medium, the Tellegen parameter κ affects the phase of a propagating electric field whereas the chiral parameter χ affects its polarization. A linearly polarized wave propagating in a Tellegen medium would then present an angle between the electric and magnetic fields equal to $\pi/2 + \vartheta$ [1] (where ϑ is a parameter characterizing the nonreciprocity of the medium). Several claims that this nonreciprocity would violate the so-called Post constraint have been proven wrong: there is no such thing as a Post constraint for actual media [2]. Furthermore, by resorting to a field transformation that redefines fields in such a way that a uniform Tellegen material in free space will look like a reciprocal isotropic medium, will cause the surrounding free space to look like a Tellegen

Received 30 September 2010, Accepted 24 November 2010, Scheduled 27 November 2010
Corresponding author: João R. Canto (joao.canto@lx.it.pt).

medium: only in uniform and unbounded media can we state that, through a field transformation, the Tellegen parameter in bi-isotropic constitutive relations vanishes and hence it cannot have any impact on wave propagation [3]. Finally, there is some experimental evidence of the effect of the nonreciprocal Tellegen magnetoelectric parameter [4].

The influence of nonreciprocity on the propagation features of closed metallic waveguides, circular rods, open slab waveguides, and others, has already been discussed in the literature [1, 5–10]. Moreover, a full-wave analysis of an H-guide containing chiral media has also been presented [11]. Similarly to the chiral case, there is no closed-form analytical solution, as in [12], to the modal analysis of an H-guide containing bi-isotropic media: the coupled modal equations, that describe the transverse electromagnetic field for such magnetoelectric isotropic media in H-guides, preclude such a closed-form analytical solution. In fact, to the authors' knowledge, no work addressing H-guides containing bi-isotropic, or specifically Tellegen media, has been published so far.

In this article, a rigorous analysis of a bi-isotropic H-guide, as shown in Figure 1, is presented. The approach is based on a transverse resonance method combined with a mode-matching technique. This work may then be considered as an extension of the method used in [11] for chiral media, in order to investigate the general bi-isotropic case by including the effect of nonreciprocity. In this building-block approach, the modal equation of a parallel-plate waveguide containing a lossless bi-isotropic medium is obtained in the first place. Then, using a mode-matching technique, a full-wave analysis of the bi-isotropic H-guide is developed. The guidance properties of this structure are then analyzed and its potential applications discussed. It is shown that, nonreciprocity introduces several changes in both the elementary structure and the H-guide. Namely, the elementary parallel-plate Tellegen waveguide can only support a set of TE modes and a set of Hybrid modes, unlike when both chirality and nonreciprocity are present (all propagating modes become hybrid). Furthermore, for the range of parameters herein considered, an increase in the nonreciprocity parameter, introduces a proportional shift in the cutoff frequencies of modes supported by the H-guide (which is not similar to the shift caused by chirality). Moreover, an increase in the nonreciprocity parameter also increases the velocities of propagating modes. Namely, for any given mode, there is a bound on the magnitude of the Tellegen parameter, beyond which the mode is at cutoff. These new features cannot be found in the corresponding reciprocal grounded chiroslabguide (e.g., [8, 13, 14]).

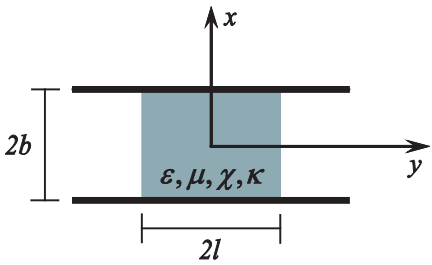

Figure 1. Bi-isotropic H-guide.

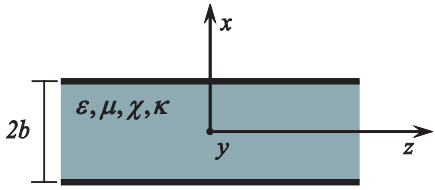

Figure 2. Bi-isotropic parallel-plate waveguide.

2. DISPERSION DIAGRAMS OF THE ELEMENTARY STRUCTURES

The first step of the building block approach, to address an H-guide filled with a bi-isotropic medium, is to obtain the modal equation of a parallel–plate waveguide, Figure 2, filled with the same medium. This elementary structure, is a closed waveguide where only discrete modes can propagate. In this section, the general case of a parallel-plate waveguide filled with a bi-isotropic medium is first addressed. Moreover, the specific case of a Tellegen medium is also analyzed. Dispersion diagrams of the modal solutions are presented for each case.

2.1. Waveguide Filled with a Bi-isotropic Medium

For bi-isotropic media, considering plane wave propagation of the form $\exp\left[i\left(\mathbf{k}\cdot\mathbf{r}-\omega t\right)\right]$, the constitutive relations can be written, in the frequency domain, as [1]

$$\mathbf{D} = \varepsilon_0\varepsilon\mathbf{E} + \sqrt{\varepsilon_0\mu_0}\xi\mathbf{H}, \tag{1a}$$

$$\mathbf{B} = \mu_0\mu\,\mathbf{H} + \sqrt{\varepsilon_0\,\mu_0}\zeta\mathbf{E}, \tag{1b}$$

where $\xi = \kappa + i\chi$ and $\zeta = \kappa - i\chi$. An unbounded bi-isotropic medium has two eigenwaves with orthogonal polarizations: a right handed circularly polarized (RCP) wave and a left handed circularly polarized (LCP) wave. One can then use the Bohren decomposition to write the total electromagnetic field in terms of these two waves (as they form an orthogonal base): $\mathbf{E} = \mathbf{E}_+ + \mathbf{E}_-$, $\mathbf{H} = \mathbf{H}_+ + \mathbf{H}_-$. The constitutive relations (1a) and (1b) can then be rewritten as,

$$\mathbf{D}_\pm = \varepsilon_0\varepsilon_\pm\mathbf{E}_\pm, \tag{2a}$$

$$\mathbf{B}_\pm = \mu_0\mu_\pm\mathbf{H}_\pm, \tag{2b}$$

where

$$\varepsilon_{\pm} = \varepsilon \left[\cos\left(\vartheta\right) \pm \chi/n\right] \exp\left(\mp i\vartheta\right), \tag{3a}$$

$$\mu_{\pm} = \mu \left[\cos\left(\vartheta\right) \pm \chi/n\right] \exp\left(\pm i\vartheta\right), \tag{3b}$$

and $\sin\left(\vartheta\right) = \kappa/\sqrt{\varepsilon\mu}$ is the parameter of nonreciprocity. Since each wave observes the Maxwell equations, one can write,

$$\nabla \times \mathbf{E}_{\pm} = i\omega\mu_0\mu_{\pm}\mathbf{H}_{\pm}, \tag{4a}$$

$$\nabla \times \mathbf{H}_{\pm} = -i\omega\varepsilon_0\varepsilon_{\pm}\mathbf{E}_{\pm}. \tag{4b}$$

For a structure layered along x and unbounded along y, one has $\nabla = \partial/\partial x\hat{\mathbf{x}} + i\beta/k_0\,\hat{\mathbf{z}}$. Choosing E_y and Z_0H_y as the supporting field components, the other fields can be written as

$$E_x^{\pm} = \frac{1}{\varepsilon_{\pm}}\frac{\beta}{k_0}Z_0H_y^{\pm}, \tag{5a}$$

$$Z_0H_x^{\pm} = -\frac{1}{\mu_{\pm}}\frac{\beta}{k_0}E_y^{\pm}, \tag{5b}$$

$$E_z^{\pm} = i\frac{1}{\varepsilon_{\pm}}\frac{1}{k_0}\frac{\partial}{\partial x}Z_0H_y^{\pm}, \tag{6a}$$

$$Z_0H_z^{\pm} = -i\frac{1}{\mu_{\pm}}\frac{1}{k_0}\frac{\partial}{\partial x}E_y^{\pm}, \tag{6b}$$

and the following wave equations are derived

$$\frac{\partial^2}{\partial x^2}\left\{\begin{array}{c} E_y^{\pm} \\ H_y^{\pm} \end{array}\right\} = -\left(n_{\pm}k_0^2 - \beta^2\right)\left\{\begin{array}{c} E_y^{\pm} \\ H_y^{\pm} \end{array}\right\}, \tag{7}$$

where $n_{\pm} = \sqrt{\varepsilon_{\pm}\mu_{\pm}} = \sqrt{\varepsilon\mu - \kappa^2} \pm \chi$. From the Bohren decomposition, the total fields are given by

$$E_y = E_y^{+} + E_y^{-}, \tag{8a}$$

$$Z_0H_y = -i\left(Y_{+}E_y^{+} + Y_{-}E_y^{-}\right), \tag{8b}$$

where $Y_{\pm} = \sqrt{\varepsilon_{\pm}/\mu_{\pm}} = \sqrt{\varepsilon/\mu}\exp\left(\mp i\vartheta\right)$, $E_y^{\pm}\left(x\right) = A_{\pm}\sin\left(h_{\pm}x + \phi\right)$ and $h_{\pm} = n_{\pm}k_0^2 - \beta^2$. Given the symmetry of the structure, the modal solutions can be split into even ($\phi = \pi/2$) and odd ($\phi = 0$) modes. The structure has two perfectly conducting planes placed at $x = \pm b$, enforcing that $E_y\left(x = \pm b\right) = 0$ and $E_z\left(x = \pm b\right) = 0$. Enforcing these boundary conditions results in the modal equations for odd and even modes, respectively,

$$n_{+}\frac{h_{-}}{k_0}\sin\left(h_{+}b\right)\cos\left(h_{-}b\right) + n_{-}\frac{h_{+}}{k_0}\cos\left(h_{+}b\right)\sin\left(h_{-}b\right) = 0, \tag{9}$$

$$n_{+}\frac{h_{-}}{k_0}\cos\left(h_{+}b\right)\sin\left(h_{-}b\right) + n_{-}\frac{h_{+}}{k_0}\sin\left(h_{+}b\right)\cos\left(h_{-}b\right) = 0. \tag{10}$$

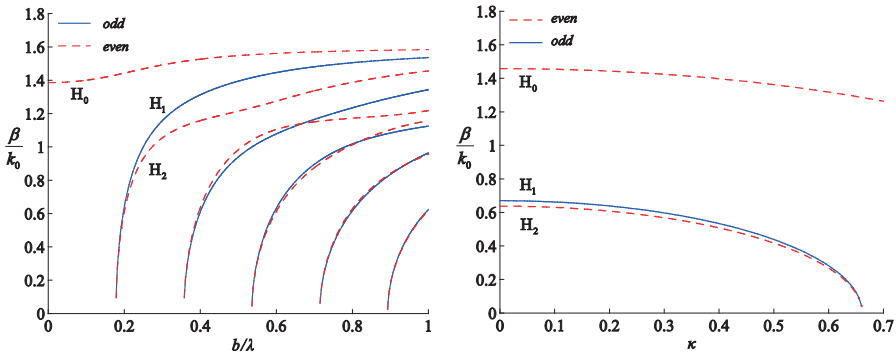

Figure 3. Parallel-plate bi-isotropic waveguide: (a) dispersion diagram ($\varepsilon = 2$, $\mu = 1$, $\chi = 0.2$ and $\kappa = 0.2$); (b) influence of the nonreciprocity parameter κ in the modal solutions ($\chi = 0.2$, $b/\lambda = 0.2$).

In Figure 3(a) the dispersion diagram of a bi-isotropic parallel-plate guide is shown, whereas in Figure 3(b) the influence of the nonreciprocity parameter in the behavior of modal solutions can be observed: an increase in the value of κ, increases the mode velocities. This causes any given mode to be at cutoff, when κ is set beyond a critical value. By setting $\kappa = 0$ into (9) and (10) the case of a waveguide filled with a chiral medium is obtained [11]. Note that, all the modal solutions supported by the bi-isotropic, reciprocal or nonreciprocal, parallel-plate waveguide are hybrid.

2.2. Waveguide Filled with a Tellegen Medium

For Tellegen media ($\chi = 0$), one has that

$$h_- = h_+ = h, \tag{11a}$$

$$n_- = n_+ = n_\kappa. \tag{11b}$$

Replacing (11a) and (11b) into (5a), (5b), (6a), (6b) and (8a), (8b), one obtains for the field components

$$E_y = (A_+ + A_-)\sin(hx + \phi), \tag{12a}$$

$$Z_0 H_y = -i\,(Y_+ A_+ - Y_- A_-)\sin(hx + \phi), \tag{12b}$$

$$E_x = -i\frac{1}{n}\frac{\beta}{k_0}(A_+ - A_-)\sin(hx + \phi), \tag{13a}$$

$$Z_0 H_x = -\frac{\beta}{k_0}\left(\frac{1}{\mu_+}A_+ + \frac{1}{\mu_-}A_-\right)\sin(hx + \phi), \tag{13b}$$

$$E_z = \frac{1}{n_\kappa}\frac{h}{k_0}\left(A_+ - A_-\right)\cos\left(hx+\phi\right), \tag{14a}$$

$$Z_0 H_z = -i\frac{h}{k_0}\left(\frac{1}{\mu_+}A_+ + \frac{1}{\mu_-}A_-\right)\cos\left(hx+\phi\right). \tag{14b}$$

Defining A_E and A_H as

$$A_E = A_+ + A_-, \tag{15a}$$

$$A_H = -i\left(Y_+ A_+ - Y_- A_-\right), \tag{15b}$$

the field components can be written as

$$E_y = A_E \sin\left(hx+\phi\right), \tag{16a}$$

$$Z_0 H_y = A_H \sin\left(hx+\phi\right), \tag{16b}$$

$$E_x = \frac{1}{n_\kappa^2}\frac{\beta}{k_0}\left(\kappa A_E + \mu A_H\right)\sin\left(hx+\phi\right), \tag{17a}$$

$$Z_0 H_x = -\frac{1}{n_\kappa^2}\frac{\beta}{k_0}\left(\varepsilon A_E + \kappa A_H\right)\sin\left(hx+\phi\right), \tag{17b}$$

$$E_z = i\frac{1}{n_\kappa^2}\frac{h}{k_0}\left(\kappa A_E + \mu A_H\right)\cos\left(hx+\phi\right), \tag{18a}$$

$$Z_0 H_z = -i\frac{1}{n_\kappa^2}\frac{h}{k_0}\left(\varepsilon A_E + \kappa A_H\right)\cos\left(hx+\phi\right). \tag{18b}$$

Again, given the symmetry of the structure, the modal solutions can be split into odd and even ($\phi = 0$ or $\phi = \pi/2$, respectively). The types of modes supported by this structure are now discussed.

2.2.1. TE Modes

In order to check for the existence of TE modes, one must enforce that $E_z(x) = 0$. From (18a), this results in

$$A_H = -\kappa/\mu A_E. \tag{19}$$

The field components can then be rewritten as

$$E_y = A_E \sin\left(hx+\phi\right), \tag{20a}$$

$$Z_0 H_y = -\frac{\kappa}{\mu}A_E \sin\left(hx+\phi\right), \tag{20b}$$

$$Z_0 H_x = -\frac{1}{\mu}\frac{\beta}{k_0}A_E \sin\left(hx+\phi\right), \tag{21a}$$

$$Z_0 H_z = -i\frac{1}{\mu}\frac{h}{k_0}A_E \cos\left(hx+\phi\right), \tag{21b}$$

and $E_x(x) = 0$. Enforcing the boundary condition $E_y(x = b) = 0$ in (20a) results in

$$\sin(hb + \phi) = 0. \tag{22}$$

The modal Equation (22) can be explicitly solved for odd and even modes respectively

$$\sin(hb) = 0 \quad \Rightarrow \quad h = \frac{m\pi}{b}, \quad m \geq 1, \tag{23}$$

$$\cos(hb) = 0 \quad \Rightarrow \quad h = \frac{\pi}{2b} + \frac{m\pi}{b}, \quad m \geq 0. \tag{24}$$

For $m = 0$ only the even mode exists, since, for the odd mode, from (16a) and (16b), $E_y = H_y = 0$, and all the field components become null everywhere.

2.2.2. TM Modes

In this section, it is shown that this structure does not support TM modes. Enforcing $H_z = 0$ in (18b) results in

$$A_H = -\varepsilon/\kappa A_E, \tag{25}$$

and the following field components are obtained

$$E_y = A_E \sin(hx + \phi), \tag{26a}$$

$$Z_0 H_y = -\frac{\varepsilon}{\kappa} A_E \sin(hx + \phi), \tag{26b}$$

$$E_x = -\frac{1}{\kappa}\frac{\beta}{k_0} A_E \sin(hx + \phi), \tag{27a}$$

$$E_z = -i\frac{1}{\kappa}\frac{h}{k_0} A_E \cos(hx + \phi). \tag{27b}$$

Enforcing the boundary condition $E_y(x = b) = 0$ in (26a) results in

$$\sin(hb + \phi) = 0. \tag{28}$$

But enforcing the boundary condition $E_z(x = b) = 0$ in (27b), and using (28), one obtains $A_E = 0$ and consequently all the field components become null everywhere. Therefore, this structure does not support TM modes.

2.2.3. Hybrid Modes

As it was verified in Section 2.2.1, it is not possible to have simultaneously $A_E \neq 0$ and $A_H \neq 0$ unless $E_z = 0$ everywhere. In fact, enforcing the boundary conditions $E_y(x = b) = 0$ and $E_z(x = b) = 0$ in (16a) and (18a) requires that $A_H = -\kappa/\mu A_E$, which leads to TE

modes. Therefore, to check for the existence of hybrid modes, only the remaining possible values for A_E and A_H must be considered: *(i)* $A_H = 0$ and $A_E \neq 0$; *(ii)* $A_E = 0$ and $A_H \neq 0$.

For case (*i*), replacing $A_H = 0$ and $A_E \neq 0$ in (16a)–(18b) results in

$$E_y = A_E \sin(hx + \phi), \tag{29a}$$

$$Z_0 H_y = 0, \tag{29b}$$

$$E_x = \frac{1}{n_\kappa^2}\frac{\beta}{k_0}\kappa A_E \sin(hx + \phi), \tag{30a}$$

$$Z_0 H_x = -\frac{1}{n_\kappa^2}\frac{\beta}{k_0}\varepsilon A_E \sin(hx + \phi), \tag{30b}$$

$$E_z = i\frac{\kappa}{n_\kappa^2}\frac{h}{k_0} A_E \cos(hx + \phi), \tag{31a}$$

$$Z_0 H_z = -i\frac{1}{n_\kappa^2}\varepsilon\frac{h}{k_0} A_E \cos(hx + \phi). \tag{31b}$$

Enforcing the boundary condition $E_y(x = b) = 0$ results in (28). But, enforcing $E_z(x = b) = 0$ in (31a) imposes that $A_E = 0$ and consequently all the fields become null everywhere. Therefore, this structure does not support modes with $A_H = 0$ and $A_E \neq 0$.

For case *(ii)*, replacing $A_E = 0$ and $A_H \neq 0$ in (16a)–(18b), results in a family of hybrid modal solutions, with the following field configuration

$$E_y = 0, \tag{32a}$$

$$Z_0 H_y = A_H \sin(hx + \phi), \tag{32b}$$

$$E_x = \frac{\mu}{n_\kappa^2}\frac{\beta}{k_0} A_H \sin(hx + \phi), \tag{33a}$$

$$Z_0 H_x = -\frac{\kappa}{n_\kappa^2}\frac{\beta}{k_0} A_H \sin(hx + \phi), \tag{33b}$$

$$E_z = i\frac{\mu}{n_\kappa^2}\frac{h}{k_0} A_H \cos(hx + \phi), \tag{34a}$$

$$Z_0 H_z = -i\frac{\kappa}{n_\kappa^2}\frac{h}{k_0} A_H \cos(hx + \phi). \tag{34b}$$

Note that, these hybrid modes cannot be written as a combination of the previously found TE modes. Also, the previous TE modes cannot be written as a combination of these hybrid modes. Enforcing the boundary condition $E_z(x = b) = 0$ in (34a), results in the modal equation,

$$\cos(hb + \phi) = 0, \tag{35}$$

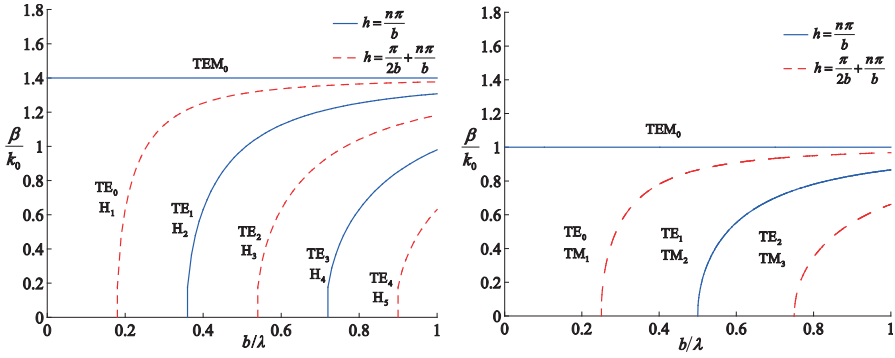

Figure 4. Dispersion diagram of a parallel-plate waveguide filled with: (a) a Tellegen medium ($\varepsilon = 2$, $\mu = 1$ and $\kappa = 0.2$); (b) air.

which leads to the same modal solutions as (23)–(24). However, with this field configuration, the odd modes are given by (24) and the even modes by (23). Setting $h = 0$, allows to obtain a TEM even mode

$$E_y = 0, \tag{36a}$$

$$Z_0 H_y = A_H, \tag{36b}$$

$$E_z = 0, \tag{36c}$$

$$Z_0 H_z = 0, \tag{37a}$$

$$E_x = \frac{\mu}{n_\kappa^2}\frac{\beta}{k_0} A_H, \tag{37b}$$

$$Z_0 H_x = -\frac{\kappa}{n_\kappa^2}\frac{\beta}{k_0} A_H. \tag{37c}$$

The dispersion diagram of a parallel-plate waveguide, with $\kappa = 0.2$, is shown in Figure 4(a). Note that, setting $\kappa = 0$ in (20a)–(21b), reduces the TE modal solutions, of the Tellegen waveguide, to the TE modes of the isotropic waveguide. Similarly, setting $\kappa = 0$ in (33a)–(34b), reduces the hybrid modes, of the Tellegen waveguide, to the TM modes of the isotropic waveguide (the TEM mode in (36a)–(37c) is also reduced to the TEM mode of the isotropic waveguide).

2.2.4. Waveguide Filled with an Isotropic Medium

When using a building block approach for the analysis of the H-guide, the external region is a parallel plate waveguide filled with air. The well known modal equations for this structure can be obtained by enforcing the boundary conditions to the field components (16a)–(18b) (with

$\kappa = 0$), which results in

$$\sin(hb) = 0 \quad \Rightarrow \quad h = \frac{k\pi}{b}, \tag{38}$$

for TE (TM) odd (even) modes and

$$\cos(hb) = 0 \quad \Rightarrow \quad h = \frac{\pi}{2b} + \frac{k\pi}{b}, \tag{39}$$

for TE (TM) even (odd) modes. For $h = 0$ a TEM mode is obtained.

For the sake of comparison, the modal solutions of an air filled parallel plate waveguide are depicted in Figure 4(b).

3. THE BI-ISOTROPIC H-GUIDE

Having solved the modal equations of the elementary structures in the previous section, the modal equation of the H-guide can now be derived. The next steps of the building block approach are addressed in separate sub-sections. First, orthogonality relations will be obtained for the modal solutions in the inner and outer regions of the H-guide. Unlike what can be done for the chiral H-guide [8] (or for the uniaxial ridge waveguide [15]), one must resort to the formalism proposed in [16]. Next, the scattering matrix of a step discontinuity at a parallel-plate waveguide is derived. A mode matching technique is then applied at the step discontinuity. Finally, a transverse resonance method is used to derive the modal equation of the H-guide. Note that, the procedures to obtain the scattering matrix at the step discontinuity, and to apply the transverse resonance method in order to obtain the modal equation of the H-guide are the same as those presented in [11]. Therefore, only the main differences in the formalism are highlighted.

3.1. Orthogonality Relations

Following [16], and defining an adjoint waveguide

$$\varepsilon^a = \varepsilon^*, \quad \mu^a = \mu^*, \quad \xi^a = \xi^*, \quad \zeta^a = \zeta^*, \tag{40}$$

and a complex inner product

$$\langle \mathbf{u}, \mathbf{u}^a \rangle = \int_I \left(u_1^* u_1^a - u_2^* u_2^a \right) dx, \tag{41}$$

it is possible to derive

$$\int_I \left(E_{x_{m*}}^* Z_0 H_{y_n}^a - Z_0 H_{x_{m*}}^* E_{y_n}^a \right) dx = \beta_m \delta_{mn}, \tag{42}$$

where $H_{x_{m*}}$, $E_{x_{m*}}$ are the field components of the original waveguide, whereas $E^a_{y_n}$ and $H^a_{y_n}$ are the field components of the adjoint waveguide (and δ_{mn} is the Kronecker delta). For the particular case of lossless media, the original and adjoint waveguides are identical [16], and (42), which is a biorthogonality relation, can be reduced to a plain orthogonality relation

$$\int_I \left(E^*_{x_m} Z_0 H_{y_n} - Z_0 H^*_{x_m} E_{y_n}\right) dx = \beta_m \delta_{mn}, \tag{43}$$

or, since the fields can be written as sums of sine and co-sine functions

$$\int_I \left(E_{x_m} Z_0 H^*_{y_n} - Z_0 H_{x_m} E^*_{y_n}\right) dx = \beta_m \delta_{mn}. \tag{44}$$

These relations will be used to derive the modal equation of the H-guide.

3.2. Scattering Matrix

In this section, the scattering matrix for oblique incidence at a step discontinuity in a parallel-plate waveguide, is presented. In order to account for oblique incidence, two coordinate systems will be considered, that of the structure (x, y', z), with $y' = y + l$, and that of the wave (x, u, v). These can be easily related, see Figure 5. In order to properly enforce the boundary conditions to the step, one must take into account that, in general, many sets of modes can propagate in either side of the step. Enforcing the boundary conditions, for the

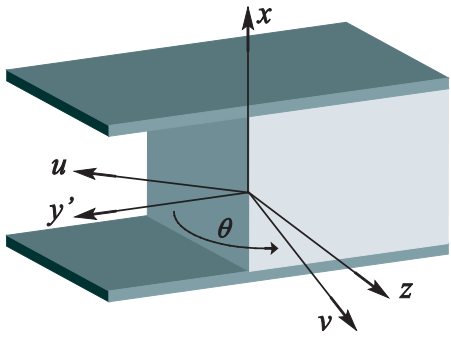

Figure 5. Step discontinuity.

tangential fields, at $y = l$, results in [11]

$$\sum_{n=1}^{+\infty} (a_n + b_n)\, E_{x_n} = \sum_{p=1}^{+\infty} c_p \bar{E}_{x_p}, \tag{45}$$

$$-\sum_{n=1}^{+\infty} (a_n - b_n) \cos(\theta_n)\, E_{u_n} + \sum_{n=1}^{+\infty} (a_n + b_n) \sin(\theta_n)\, E_{v_n}$$

$$= \sum_{p=1}^{+\infty} c_p \left[-\cos\left(\bar{\theta}_p\right) \bar{E}_{u_p} + \sin\left(\bar{\theta}_p\right) \bar{E}_{v_p} \right], \tag{46}$$

$$\sum_{n=1}^{+\infty} (a_n + b_n)\, Z_0 H_{x_n} = \sum_{p=1}^{+\infty} c_p Z_0 \bar{H}_{x_p}, \tag{47}$$

$$-\sum_{n=1}^{+\infty} (a_n - b_n) \cos(\theta_n)\, Z_0 H_{u_n} + \sum_{n=1}^{+\infty} (a_n + b_n) \sin(\theta_n)\, Z_0 H_{v_n}$$

$$= \sum_{p=1}^{+\infty} c_p \left[-\cos\left(\bar{\theta}_p\right) Z_0 \bar{H}_{u_p} + \sin\left(\bar{\theta}_p\right) Z_0 \bar{H}_{v_p} \right], \tag{48}$$

where the notation $\bar{\mathbf{E}}$, $\bar{\mathbf{H}}$ is used whenever fields are defined in the external region.

3.3. Mode-matching

In order to derive a matrix equation from the boundary conditions it is first necessary to implement a mode matching technique at the step discontinuity. Applying (43) to each side of the step, it is possible to obtain a normalized field amplitude for each mode

$$O_{mn} = \int_{-b}^{b} \left(E^*_{x_m} Z_0 H_{y_n} - Z_0 H^*_{x_m} E_{y_n} \right) dx = \frac{\beta_m}{k_0} \delta_{mn}, \tag{49}$$

$$\bar{O}_{mn} = \int_{-b}^{b} \left(\bar{E}^*_{x_m} Z_0 \bar{H}_{y_n} - Z_0 \bar{H}^*_{x_m} \bar{E}_{y_n} \right) dx = \frac{\bar{\beta}_m}{k_0} \delta_{mn}. \tag{50}$$

Multiplying (45) by $Z_0 \bar{H}^*_{u_m}$ and subtracting from (47) multiplied by $\bar{E}^*_{u_m}$ results in

$$\sum_{n=1}^{+\infty} (a_n + b_n) \left[E_{x_n} Z_0 \bar{H}^*_{u_m} - Z_0 H_{x_n} \bar{E}^*_{u_m} \right] = \sum_{p=1}^{+\infty} c_p \left[\bar{E}_{x_p} Z_0 \bar{H}^*_{u_m} - Z_0 \bar{H}_{x_p} \bar{E}^*_{u_m} \right]. \tag{51}$$

Now, integrating (51) between $-b$ and b, and using (44), the amplitude coefficients of the transmitted waves are obtained

$$c_m = \frac{1}{\bar{\beta}_m} \sum_{n=1}^{\infty} (a_n + b_n) P_{nm}, \tag{52}$$

where

$$P_{nm} = \int_{-b}^{b} \left(E_{x_n} Z_0 \bar{H}^*_{u_m} - Z_0 H_{x_n} \bar{E}^*_{u_m} \right) dx. \tag{53}$$

On the other hand, multiplying (48) by $\bar{E}^*_{x_m}$ and subtracting from (46) multiplied by $Z_0 \bar{H}^*_{x_m}$, one arrives at

$$\begin{aligned} & -\sum_{n=1}^{\infty} (a_n - b_n) \cos\theta_n \left(\bar{E}^*_{x_m} Z_0 H_{u_n} - Z_0 \bar{H}^*_{x_m} E_{u_n} \right) \\ & + \sum_{n=1}^{\infty} (a_n + b_n) \sin\theta_n \left(\bar{E}^*_{x_m} Z_0 H_{v_n} - Z_0 \bar{H}^*_{x_m} E_{v_n} \right) \\ = & \sum_{p=1}^{\infty} c_p \left[-\cos\bar{\theta}_p \left(\bar{E}^*_{x_m} Z_0 \bar{H}_{u_p} - Z_0 \bar{H}^*_{x_m} \bar{E}_{u_p} \right) \right. \\ & \left. + \sin\bar{\theta}_p \left(\bar{E}^*_{x_m} Z_0 \bar{H}_{v_p} - Z_0 \bar{H}^*_{x_m} \bar{E}_{v_p} \right) \right]. \end{aligned} \tag{54}$$

Finally, integrating (54) between $-b$ and b, taking into account (43) and (52), it is possible to obtain

$$\begin{aligned} & -\sum_{n=1}^{\infty} (a_n - b_n) \cos\theta_n Q_{mn} + \sum_{n=1}^{\infty} (a_n + b_n) \sin\theta_n R_{mn} \\ = & -\cos\bar{\theta}_m \sum_{n=1}^{\infty} (a_n + b_n) P_{nm} + \sum_{p=1}^{\infty} \frac{1}{\bar{\beta}_p} \sin\bar{\theta}_p S_{mp} \sum_{n=1}^{\infty} (a_n + b_n) P_{np}, \end{aligned} \tag{55}$$

where

$$Q_{mn} = \int_{-b}^{b} \left(\bar{E}^*_{x_m} Z_0 H_{u_n} - Z_0 \bar{H}^*_{x_m} E_{u_n} \right) dx, \tag{56}$$

$$R_{mn} = \int_{-b}^{b} \left(\bar{E}^*_{x_m} Z_0 H_{v_n} - Z_0 \bar{H}^*_{x_m} E_{v_n} \right) dx, \tag{57}$$

$$S_{mp} = \int_{-b}^{b} \left(\bar{E}^*_{x_m} Z_0 \bar{H}_{v_p} - Z_0 \bar{H}^*_{x_m} \bar{E}_{v_p} \right) dx. \tag{58}$$

It is possible to write (55) in a simpler matrix form [11]

$$(\mathbf{C}+\mathbf{D})\cdot\mathbf{a}=(\mathbf{C}-\mathbf{D})\cdot\mathbf{b}, \tag{59}$$

where

$$\mathbf{a}=[a_1,a_2,\ldots,a_n]^{\mathrm{T}}, \quad \mathbf{b}=[b_1,b_2,\ldots,b_n]^{\mathrm{T}}, \tag{60}$$

$$C_{mn}=\cos\theta_n Q_{mn}, \tag{61}$$

$$D_{mn}=-\sin\theta_n R_{mn}-\cos\bar{\theta}_m P_{nm}+\sum_{p=1}^{\infty}\frac{1}{\bar{\beta}_p}\sin\bar{\theta}_p S_{mp}P_{np}. \tag{62}$$

The analytical calculations to explicitly obtain the internal products defined in (49), (50), (56)–(58) are presented in Appendix A.

3.4. Transverse Resonance

In this section, the transverse resonance method is applied to derive the modal equation of the H-guide. From Figure 1, one can identify $y=0$ as a symmetry plane, hence, the propagating modes can be split into odd and even solutions. Defining

$$\mathbf{L}=\mathrm{diag}\left(e^{i2k_{y_1}l},\ e^{i2k_{y_2}l},\ \ldots,\ e^{i2k_{y_n}l}\right), \tag{63}$$

it is possible to obtain, $\mathbf{a}=-\mathbf{L}\cdot\mathbf{b}$ and $\mathbf{a}=\mathbf{L}\cdot\mathbf{b}$. One can then define a reflection matrix, such that, $\overleftarrow{\mathbf{\Gamma}}=\Gamma\,\mathbf{L}$, where $L=\pm1$ for even and odd modes respectively, thereby arriving at

$$\mathbf{a}=\overleftarrow{\mathbf{\Gamma}}\cdot\mathbf{b}. \tag{64}$$

Replacing (64) into (59), it is possible to write the modal equation for the bi-isotropic H-guide as

$$\det\left[\mathbf{I}+\frac{\mathbf{D}\cdot\left(\overleftarrow{\mathbf{\Gamma}}+\mathbf{I}\right)}{\mathbf{C}\cdot\left(\overleftarrow{\mathbf{\Gamma}}-\mathbf{I}\right)}\right]=0. \tag{65}$$

Numerical results of this modal equation are presented and discussed in the following section.

3.5. Numerical Results

In this section, some numerical results are presented for the case of a Tellegen H-guide and for the most general case of a bi-isotropic H-guide. The numerical results have been obtained taking into account the contribution of all the elementary modes above cutoff for each region.

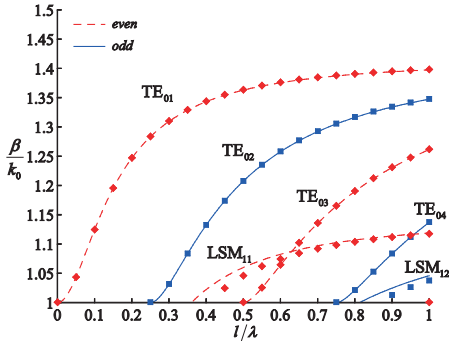

Figure 6. Dispersion diagram of an isotropic H-guide ($\varepsilon = 2$, $\mu = 1$ and $b/\lambda = 0.3$).

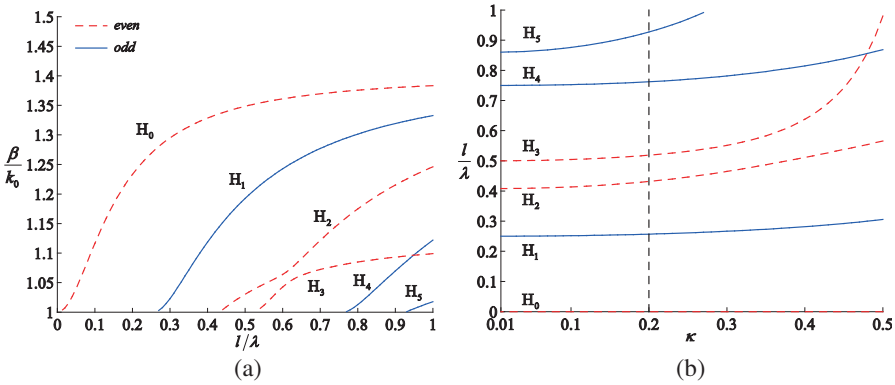

Figure 7. Tellegen H-guide ($\varepsilon = 2$, $\mu = 1$, $b/\lambda = 0.3$): (a) dispersion diagram ($\kappa = 0.2$); (b) operational diagram.

To assess the present method, the dispersion diagram of an isotropic H-guide has been obtained and is presented in Figure 6 (using square dots) and compared with the numerical results of the modal equation (full lines) which, in this case, can be expressed as an exact closed form expression. The agreement is very good for the TE$_{op}$ modes and quite good for the hybrid modes improving as the frequency increases above cutoff.

The dispersion diagram of a Tellegen H-guide is presented in Figure 7(a). Given that the modes are all hybrid, they are numbered as H_n, starting from the mode with the lowest cutoff frequency. As for the chiral H-guide [11], a mode with zero cutoff frequency exists and mode coupling effects (e.g., modes H_2 and H_3) are present.

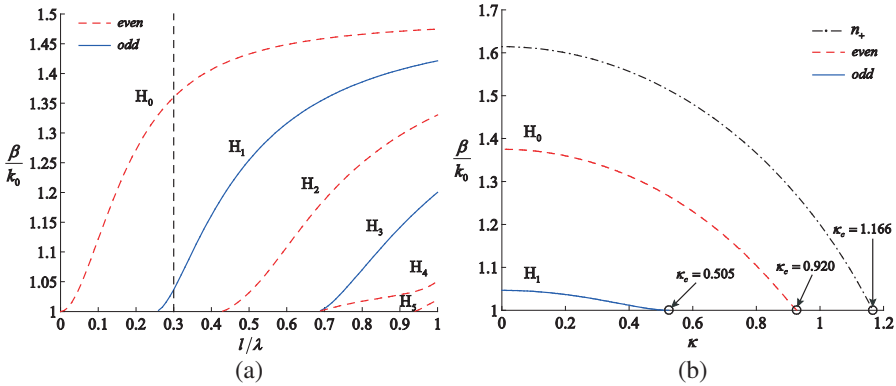

Figure 8. Bi-isotropic H-guide ($\chi = 0.2$, $\varepsilon = 2$, $\mu = 1$, $b/\lambda = 0.3$): (a) dispersion diagram ($\kappa = 0.2$); (b) influence of the nonreciprocity parameter κ in the modal solutions H_0 and H_1 ($\chi = 0.2$ and $l/\lambda = 0.3$).

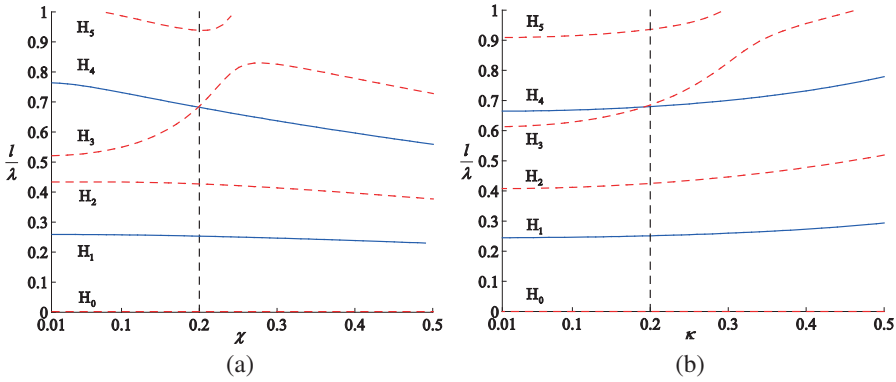

Figure 9. Operational diagrams of a bi-isotropic H-guide ($\varepsilon = 2$, $\mu = 1$, $b/\lambda = 0.3$): (a) $\kappa = 0.2$; (b) $\chi = 0.2$.

The operational diagram depicted in Figure 7(b) shows the effect of the non reciprocity parameter on the cutoff frequency of the guided modes (the vertical dashed line corresponds to $\kappa = 0.2$, as used in the numerical calculations for the dispersion diagram). For this set of parameters, the increase of the value of κ increases the cutoff frequencies which seems to be a different effect as caused by the chirality parameter [11].

The dispersion diagram for a bi-isotropic H-guide is presented in Figure 8(a). Choosing $l/\lambda = 0.3$, Figure 8(b) shows the effect of the nonreciprocity parameter on the values of the propagation constants for

the first two modes H_0 and H_1 (n_+ is added for the sake of comparison): an increase in the value of κ, increases the mode velocities. In fact, a critical value of the non-reciprocity parameter, κ_c, can be defined such that a mode reaches cutoff for $\kappa > \kappa_c$. This result is similar to that obtained in section two for the elementary structure — the bi-isotropic parallel plate waveguide. Moreover, this effect has been reported to occur in waveguides containing anisotropic media [17], whereas in our case, this is observed in an isotropic non-reciprocal waveguide. The operational diagrams for this structure are depicted in Figures 9(a) and 9(b), where one of the κ/χ parameters has been fixed, with the same values used in Figure 8(a).

4. CONCLUDING REMARKS

A rigorous analysis of lossless bi-isotropic and Tellegen H-guides has been presented using a building block approach and the transverse resonance method combined with a mode matching technique. In the reciprocal limit of our general approach, one obtains the results presented in [11]. The effects of nonreciprocity were then analyzed in detail. Namely, it was shown that, in the Tellegen limit, the elementary parallel-plate waveguide can only support a set of TE modes and a set of Hybrid modes. Moreover, when both chirality and nonreciprocity are present, all propagating modes are hybrid (similarly to the chiral limit). Dispersion and operational diagrams, for the H-guides, are then presented, and the effects of the nonreciprocity and chirality parameters discussed. In was shown that, for this range of parameters, an increase in the nonreciprocity parameter, introduces a proportional shift in the cutoff frequencies (which seems to be a different effect than the one caused by chirality). Moreover, it was observed that, an increase in the nonreciprocity parameter also increases the propagating mode velocities. Moreover, for any propagating mode, there is a bound on the magnitude of the Tellegen parameter beyond which that mode is at cutoff. The results put in evidence that new degrees of freedom can be explored for the design of devices based in these waveguides.

ACKNOWLEDGMENT

This work has been partially funded by the Foundation for Science and Technology, Portugal.

APPENDIX A. MODE-MATCHING COEFFICIENTS

In this appendix, the coefficients required for the application of the mode matching technique are explicitly obtained. In Section A.1, the specific case of a Tellegen H-guide, i.e., $\chi = 0$, is addressed. The field components are presented and the mode matching coefficients obtained through the internal products previously defined. In Section A.2, the same is obtained but for the more general case of a bi-isotropic H-guide.

A.1. Tellegen H-guide

In order to properly obtain the mode matching coefficients, it is necessary to consider the field components of the modal solutions, inside and outside the slab. As it can be seen from section two, a parallel-plated Tellegen waveguide supports odd and even TE modes, hybrid modes, and a fundamental TEM mode, with $h = 0$. It is important to recall that this formalism only allows to address surface modes, hence h is real or purely imaginary. Furthermore

$$\int_{-b}^{b} \sin(hx)\cos\left(\bar{h}x\right) dx = 0, \tag{A1}$$

holds for any values of h and $\bar{h}$.

The following relations will be used when explicitly obtaining coefficients

$$\int_{-b}^{b} \sin(hx)\sin\left(\bar{h}x\right) dx = 2\frac{\bar{h}\cos\left(\bar{h}b\right)\sin(hb) - h\cos(hb)\sin\left(\bar{h}b\right)}{h^2 - \bar{h}^2}, \tag{A2}$$

$$\int_{-b}^{b} \cos(hx)\cos\left(\bar{h}x\right) dx = 2\frac{h\cos\left(\bar{h}b\right)\sin(hb) - \bar{h}\cos(hb)\sin\left(\bar{h}b\right)}{h^2 - \bar{h}^2}, \tag{A3}$$

which reduce to

$$\int_{-b}^{b} \sin^2(hx + \phi)\, dx = b - \frac{\cos(2\phi)\sin(2hb)}{2h}, \tag{A4}$$

for $h = \bar{h}$. The mode matching coefficients, which are different for each set of modes that the Tellegen waveguide supports, can now be obtained. When the modal solutions, on the Tellegen region, are of

the TE type, one can arrive at

$$P_{nm} = \frac{1}{\mu}\frac{\beta_n}{k_0} A_{E_n} \bar{A}^*_m \int_{-b}^{b} \sin^*\left(\bar{h}_m x + \bar{\phi}_m\right) \sin\left(h_n x + \phi_n\right) dx, \tag{A5}$$

$$Q_{mn} = \frac{\bar{\beta}_m}{k_0}\left(\frac{1}{\bar{\mu}}\bar{A}^*_m A_{E_n} - \frac{1}{\bar{\varepsilon}}\frac{\kappa}{\mu}\bar{B}^*_m A_{E_n}\right) \int_{-b}^{b} \sin^*\left(\bar{h}_m x + \bar{\phi}_m\right) \sin\left(h_n x + \phi_n\right) dx, \tag{A6}$$

$$R_{mn} = -i\frac{1}{\mu}\frac{1}{\bar{\varepsilon}}\frac{\bar{\beta}_m}{k_0}\frac{h_n}{k_0}\bar{B}^*_m A_{E_n} \int_{-b}^{b} \sin^*\left(\bar{h}_m x + \bar{\phi}_m\right) \cos(h_n x + \phi_n) dx, \tag{A7}$$

$$S_{mp} = i\frac{1}{\bar{\varepsilon}\,\bar{\mu}}\frac{\bar{\beta}_m}{k_0}\frac{\bar{h}_p}{k_0}\left(\bar{A}^*_m \bar{B}_p - \bar{B}^*_m \bar{A}_p\right) \int_{-b}^{b} \sin^*\left(\bar{h}_m x + \bar{\phi}_m\right) \cos\left(\bar{h}_p x + \bar{\phi}_p\right) dx. \tag{A8}$$

Moreover, from the orthogonality relations, one also obtains

$$\bar{O}_{mn} = \frac{\bar{\beta}_m}{k_0}\left(\bar{B}^*_m \bar{B}_n \frac{1}{\bar{\varepsilon}} + \bar{A}^*_m \bar{A}_n \frac{1}{\bar{\mu}}\right) \int_{-b}^{b} \sin^*\left(\bar{h}_m x + \bar{\phi}_m\right) \sin\left(\bar{h}_n x + \bar{\phi}_n\right) dx = \frac{\bar{\beta}_m}{k_0}\delta_{mn}, \tag{A9}$$

$$O_{mn} = \frac{1}{\mu}\frac{\beta_m}{k_0} A^*_{E_m} A_{E_n} \int_{-b}^{b} \sin^*\left(h_m x + \phi_m\right) \sin\left(h_n x + \phi_n\right) dx = \frac{\beta_m}{k_0}\delta_{mn}, \tag{A10}$$

from where it can be concluded that

$$m = n \;\Rightarrow\; \begin{cases} TE, & \left|\bar{A}\right|^2 = \dfrac{\bar{\mu}}{\int_{-b}^{b} \sin^*\left(\bar{h}_m x + \bar{\phi}_m\right) \sin\left(\bar{h}_n x + \bar{\phi}_n\right) dx} \\ TM, & \left|\bar{B}\right|^2 = \dfrac{\bar{\varepsilon}}{\int_{-b}^{b} \sin^*\left(\bar{h}_m x + \bar{\phi}_m\right) \sin\left(\bar{h}_n x + \bar{\phi}_n\right) dx} \end{cases}, \tag{A11}$$

$$m = n \;\Rightarrow\; |A_E|^2 = \frac{\mu}{\int\limits_{-b}^{b} \sin^*(hx+\phi)\sin(hx+\phi)\,dx}. \quad \text{(A12)}$$

When the modal solutions, on the Tellegen region, are hybrid, one obtains

$$P_{nm} = \frac{1}{n_\kappa^2}\frac{\beta_n}{k_0} A_{H_n}\left(\mu\bar{B}_m^* + \kappa\bar{A}_m^*\right)\int\limits_{-b}^{b} \sin(h_n x+\phi_n)\sin^*\left(\bar{h}_m x+\bar{\phi}_m\right)dx, \quad \text{(A13)}$$

$$R_{mn} = i\frac{1}{n_\kappa^2}\frac{\bar{\beta}_m}{k_0}\frac{h_n}{k_0}\left(\bar{A}_m^*\frac{\mu}{\bar{\mu}} - \bar{B}_m^*\frac{\kappa}{\bar{\varepsilon}}\right)\int\limits_{-b}^{b} \sin^*\left(\bar{h}_m x+\bar{\phi}_m\right)\cos(h_n x+\phi_n)dx, \quad \text{(A14)}$$

$$Q_{mn} = \frac{1}{\bar{\varepsilon}}\frac{\bar{\beta}_m}{k_0} A_{H_n}\bar{B}_m^* \int\limits_{-b}^{b} \sin^*\left(\bar{h}_m x+\bar{\phi}_m\right)\sin\left(h_n x+\phi_n\right)dx, \quad \text{(A15)}$$

Since,

$$O_{mn} = \frac{\mu}{n_\kappa^2}\frac{\beta_m}{k_0} A_{H_m}^* A_{H_n}\int\limits_{-b}^{b} \sin^*(h_m x+\phi_m)\sin(h_n x+\phi_n)dx = \frac{\beta_m}{k_0}\delta_{mn}, \quad \text{(A16)}$$

one has,

$$m = n \quad \Rightarrow \quad |A_H|^2 = \frac{n_\kappa^2}{\mu\int\limits_{-b}^{b} \sin^*\left(h_m x+\phi_m\right)\sin\left(h_n x+\phi_n\right)dx}. \quad \text{(A17)}$$

Note that, S_{mp} and $\bar{O}_{mn}$ are the same as in the previous case. For the TEM modal solution on the Tellegen waveguide, i.e., for $h = 0$, one has that $R_{mn} = 0$, (S_{mp} and $\bar{O}_{mn}$ are again the same) and

$$P_{nm} = \frac{1}{n_\kappa^2}\frac{\beta_n}{k_0} A_{H_n}\left(\mu\bar{B}_m^* + \kappa\bar{A}_m^*\right)\int\limits_{-b}^{b} \sin^*\left(\bar{h}_m x+\bar{\phi}_m\right)dx, \quad \text{(A18)}$$

$$Q_{mn} = \frac{1}{\bar{\varepsilon}}\frac{\bar{\beta}_m}{k_0} A_{H_n}\bar{B}_m^* \int\limits_{-b}^{b} \sin^*\left(\bar{h}_m x+\bar{\phi}_m\right)dx. \quad \text{(A19)}$$

Finally, taking into account

$$O_{mn} = \frac{\mu}{n_\kappa^2}\frac{\beta_m}{k_0} A_{H_m}^* A_{H_n}\int\limits_{-b}^{b} dx = \frac{\beta_m}{k_0}\delta_{mn}, \quad \text{(A20)}$$

one can obtain,

$$m = n \quad \Rightarrow \quad |A_H|^2 = \frac{n_\kappa^2}{2\mu b}. \tag{A21}$$

A.2. Bi-isotropic H-guide

In order to obtain the mode matching coefficients, the field components, as shown in section two and (A1)–(A4) are required. Again, S_{mp} and $\bar{O}_{mn}$ are the same as in the previous cases. Accordingly, and after some algebra, one arrives at the following expressions for the mode matching coefficients,

$$P_{nm} = A_{+n}\frac{\beta_n}{k_0}\left(\bar{A}_m^*\frac{1}{\mu_+} - i\bar{B}_m^*\frac{1}{n_+}\right)\int_{-b}^{b}\sin(h_{+n}x+\phi_n)\sin^*\left(\bar{h}_m x+\bar{\phi}_m\right)dx$$

$$-R_n A_{+n}\frac{\beta_n}{k_0}\left(\bar{A}_m^*\frac{1}{\mu_-} + i\bar{B}_m^*\frac{1}{n_-}\right)\int_{-b}^{b}\sin(h_{-n}x+\phi_n)\sin^*\left(\bar{h}_m x+\bar{\phi}_m\right)dx, \tag{A22}$$

$$Q_{mn} = A_{+n}\frac{\bar{\beta}_m}{k_0}\left(\bar{A}_m^*\frac{1}{\bar{\mu}} - i\bar{B}_m^*\frac{1}{\bar{\varepsilon}}Y_+\right)\int_{-b}^{b}\sin^*\left(\bar{h}_m x+\bar{\phi}_m\right)\sin\left(h_{+n}x+\phi_n\right)dx$$

$$-R_n A_{+n}\frac{\bar{\beta}_m}{k_0}\left(\bar{A}_m^*\frac{1}{\bar{\mu}} + i\bar{B}_m^*\frac{1}{\bar{\varepsilon}}Y_-\right)$$

$$\int_{-b}^{b}\sin^*\left(\bar{h}_m x+\bar{\phi}_m\right)\sin\left(h_{-n}x+\phi_n\right)dx, \tag{A23}$$

$$R_{mn} = A_{+n}\frac{\bar{\beta}_m}{k_0}\frac{h_{+n}}{k_0}\left(\bar{A}_m^*\frac{1}{\bar{\mu}}\frac{1}{n_+} - i\bar{B}_m^*\frac{1}{\bar{\varepsilon}}\frac{1}{\mu_+}\right)$$

$$\int_{-b}^{b}\cos\left(h_{+n}x+\phi_n\right)\sin^*\left(\bar{h}_m x+\bar{\phi}_m\right)dx$$

$$+A_{+n}R_n\frac{\bar{\beta}_m}{k_0}\frac{h_{-n}}{k_0}\left(\bar{A}_m^*\frac{1}{\bar{\mu}}\frac{1}{n_-} + i\bar{B}_m^*\frac{1}{\bar{\varepsilon}}\frac{1}{\mu_-}\right)$$

$$\int_{-b}^{b}\cos\left(h_{-n}x+\phi_n\right)\sin^*\left(\bar{h}_m x+\bar{\phi}_m\right)dx, \tag{A24}$$

where

$$R_m = \frac{\sin\left(h_{+m}b + \phi_m\right)}{\sin\left(h_{-m}b + \phi_m\right)}. \tag{A25}$$

Finally, taking into account that

$$O_{mn}=A^*_{+m}A_{+n}\frac{\beta_m}{k_0}\left\{\int_{-b}^{b}[Y_+ f_{+n}(x)+R_n Y_- f_{-n}(x)]\left[\frac{1}{n^*_+}f^*_{+m}(x)+\frac{R^*_m}{n^*_-}f^*_{-m}(x)\right]\right.$$
$$\left.+\left[\frac{1}{\mu^*_+}f^*_{+m}(x)-\frac{R^*_m}{\mu^*_-}f^*_{-m}(x)\right][f_{+n}(x)-R_n f_{-n}(x)]dx\right\}=\frac{\beta_m}{k_0}\delta_{mn}, \tag{A26}$$

where

$$f_{\pm m}\left(x\right) = \sin\left(h_{\pm m}x + \phi_m\right), \tag{A27}$$

one can obtain, for $m = n$,

$$\frac{1}{|A_+|^2} = \left(\frac{Y_+}{n^*_+}+\frac{1}{\mu^*_+}\right)\int_{-b}^{b} f^*_+(x)f_+(x)dx + R\left(\frac{Y_-}{n^*_+}-\frac{1}{\mu^*_+}\right)\int_{-b}^{b} f^*_+(x)f_-(x)dx$$
$$+R^*\left(\frac{Y_+}{n^*_-}-\frac{1}{\mu^*_-}\right)\int_{-b}^{b} f^*_-(x)f_+(x)dx$$
$$+|R|^2\left(\frac{Y_-}{n^*_-}+\frac{1}{\mu^*_-}\right)\int_{-b}^{b} f^*_-(x)f_-(x)dx. \tag{A28}$$

REFERENCES

1. Lindell, I. V., A. H. Sihvola, S. A. Tretyakov, and A. J. Viitanen, *Electromagnetic Waves in Chiral and Bi-isotropic Media*, Artech House, Boston, MA, 1994.
2. Hehl, F. W. and Y. N. Obukhov, "Linear media in classical electrodynamics and the Post constraint," *Phys. Lett. A*, Vol. 334, 249–259, 2005.
3. Serdyukov, A., I. Semchenko, S. Tretyakov, and A. Sihvola, *Electromagnetics of Bi-anisotropic Materials: Theory and Applications*, Gordon and Breach, Amsterdam, 2001.
4. Tretyakov, S. A., S. I. Maslovski, I. S. Nefedov, A. J. Viitanen, P. A. Belov, and A. Sanmartin, "Artificial Tellegen particle," *Electromagnetics*, Vol. 23, No. 8, 665–680, 2003.

5. Paiva, C. R., A. L. Topa, and A. M. Barbosa, "Novel propagation features of dielectric planar chirowaveguides due to nonreciprocity," *Microwave Opt. Technol. Lett.*, Vol. 6, No. 3, 182–185, Mar. 1993.
6. Ioannidis, A. D., G. Kristensson, and D. Sjöberg, "On the dispersion equation for a homogeneous, bi-isotropic waveguide of arbitrary cross-section," *Microwave Opt. Technol. Lett.*, Vol. 51, No. 11, 2701–2705, 2009.
7. Ioannidis, A. D., G. Kristensson, and D. Sjöberg, "The propagation problem in a bi-isotropic waveguide," *Progress In Electromagnetics Research B*, Vol. 19, 21–40, 2010.
8. Shi, Y., X. Luan, J. Qin, C. J. Lv, and C. H. Liang, "Multilevel Green's function interpolation method solution of volume/surface integral equation for mixed conducting/bi-isotropic objects," *Progress In Electromagnetics Research*, Vol. 107, 239–252, 2010.
9. Shi, Y. and C. H. Chan, "Solution to electromagnetic scattering by bi-isotropic media using multilevel Green's function interpolation method," *Progress In Electromagnetics Research*, Vol. 97, 259–274, 2009.
10. Hasar, U. C. and O. Simsek, "A simple approach for evaluating the reciprocity of materials without using any calibration standard," *Progress In Electromagnetics Research*, Vol. 91, 139–152, 2009.
11. Topa, A. L., C. R. Paiva, and A. M. Barbosa, "Electromagnetic wave propagation in chiral H-guides," *Progress In Electromagnetics Research*, Vol. 103, 285–303, 2010.
12. Topa, A. L., C. R. Paiva, and A. M. Barbosa, "Novel propagation features of double negative H-guides and H-guide couplers," *Microwave Opt. Technol. Lett.*, Vol. 47, No. 2, 185–190, Oct. 2005.
13. Wu, Z., B. Q. Zeng, and S. Zhong, "A double-layer chiral metamaterial with negative index," *Journal of Electromagnetic Waves and Applications*, Vol. 24, No. 7, 983–992, 2010.
14. Dong, J., "Surface wave modes in chiral negative refraction grounded slab waveguides," *Progress In Electromagnetics Research*, Vol. 95, 153–166, 2009.
15. Topa, A. L., C. R. Paiva, and A. M. Barbosa, "Guidance and leakage behavior of uniaxial ridge waveguides," *Journal of Electromagnetic Waves and Applications*, Vol. 23, No. 13, 1675–1684, 2009.
16. Topa, A. L., C. R. Paiva, and A. M. Barbosa, "New biorthogonality relations for inhomogeneous biisotropic planar waveguides," *IEEE Trans. Microwave Theory Tech.*, Vol. 42,

No. 4, 629–634, Apr. 1994.

17. Paiva, C. R. and A. M. Barbosa, "An analytical approach to stratified waveguides with anisotropic layers in the longitudinal or polar configurations," *Journal of Electromagnetic Waves and Applications*, Vol. 4, No. 1, 75–93, Apr. 1990.